

Energy Arbitrage with Thermostatically Controlled Loads

Johanna L. Mathieu, Maryam Kamgarpour, John Lygeros, and Duncan S. Callaway

Abstract—We investigate the potential for aggregations of residential thermostatically controlled loads (TCLs), such as air conditioners, to arbitrage intraday wholesale electricity market prices via non-disruptive direct load control. Since wholesale electricity prices reflect power system conditions, arbitrage provides a service to the grid, helping to balance real-time supply and demand. While previous work on the energy arbitrage problem has used simple energy storage models, we use high fidelity TCL-specific models which allow us to understand and quantify the full capabilities and constraints of these time-varying systems. We explore two optimization/control frameworks for solving the arbitrage problem, both based on receding horizon linear programming. Since we find that the first approach requires significant computation, we develop a second approach involving decomposition of the optimal control problem into separate optimization and control problems. Simulation results show that TCLs could save on the order of 10% of wholesale energy costs via arbitrage, with savings decreasing with price forecast error.

I. INTRODUCTION

With increasing deployment of smart grid infrastructure, power systems operations and electricity markets are changing. Instead of electricity supply following demand, portions of demand can now be molded to fit supply [1], which is especially important in power systems with high penetrations of intermittent renewable resources such as wind and solar [2]. There are many mechanisms for demand-side elasticity including direct load control, interruptible load management, and energy/capacity bidding demand response (DR) programs, in which loads are compensated for curtailments. In dynamic electricity pricing programs, prices vary throughout the day or on key days of the year. These DR programs pass some price information from the wholesale (supply-side) to the retail (demand-side) electricity market, but are generally limited to large industrial and commercial customers. In the residential sector, retail rates are often flat throughout the day, though some regions use time-of-use retail rates. Time-varying rates encourage electric loads to arbitrage, i.e., buy more energy when electricity prices are low, and less when they are high.

Manuscript received October 29, 2012, revised April 23, 2013. J.L. Mathieu and D.S. Callaway were supported by the PSERC Future Grid Initiative. M. Kamgarpour and J. Lygeros were supported by the European Commission under the MoVeS project FP7-ICT-2009-257005.

J. L. Mathieu is with the Power System Laboratory at ETH Zürich, ETL G 24.2, Physikstrasse 3, CH-8092 Zürich, Switzerland jmathieu@eeh.ee.ethz.ch

M. Kamgarpour and J. Lygeros are with the Automatic Control Laboratory at ETH Zürich, Switzerland {mkamgar, lygeros}@control.ee.ethz.ch

D. S. Callaway is with the Energy and Resources Group at the University of California, Berkeley, USA dcal@berkeley.edu

One way to improve demand-side elasticity would be to allow load aggregators to buy electricity directly from wholesale electricity markets.¹ Since wholesale electricity prices reflect power system conditions, loads arbitraging wholesale energy prices could provide a service to the grid, helping balance supply and demand in real-time. Aggregations of residential thermostatically controlled loads (TCLs), such as air conditioners, electric space heaters, and refrigerators, are suitable for short timescale (e.g., minutes) energy arbitrage because they operate within a hysteretic dead-band and therefore have “slack” [3]. This means that as long as they operate within their dead-band they provide the service requested by the electricity consumer, but their specific position within the dead-band can be manipulated to achieve some system-wide objective. Load control within existing dead-bands is referred to as “non-disruptive.” Load aggregations can be thought of as similar to energy storage devices with an energy reservoir, state of charge, losses, and power/energy capacities [4]. However, these values are time-varying for load aggregations consisting of TCLs such as air conditioners and electric space heaters whose consumption varies as a function of outdoor air temperature. Therefore, we can think of them as *time-varying thermal batteries*.

The objective of this paper is to understand if non-disruptive direct load control of TCL aggregations could be used to arbitrage intra-hour electricity market prices. A key contribution is the development and comparison of models and optimal control frameworks tailored specifically to aggregations of TCLs. We use these models and frameworks to quantify the magnitude of energy cost savings in order to understand if the savings would cover the costs associated with communications, infrastructure, maintenance, etc. required for non-disruptive control. We assume a load aggregator would use models and forecasts to compute optimal control trajectories and then coordinate control responses by sending direct control signals to TCLs; hence individual TCLs would not directly face time-varying prices. While the energy arbitrage problem has been investigated by a number of researchers [5], [6], [7], [8], [9], [10], past research has used either generic energy storage models or models tailored to specific types of energy storage devices, such as compressed air units and batteries. These models do not take into account the specific capabilities and constraints of TCL aggregations, especially the time-varying nature of the resource.

We are primarily interested in determining an *upper bound* of the energy cost savings to determine if they are sufficient

¹Loads would also need to pay electricity transmission and distribution costs, which are currently wrapped into retail rates.

to cover the costs associated with the scheme. Therefore, our optimization/control formulations assume full state measurements and perfect price and temperature forecasts; however, in simulation we investigate situations in which we do not have perfect forecasts and show that this leads to reductions in savings. Additionally, we assume that energy arbitrage does not affect market prices implying TCL arbitrage comprises a small fraction of the market. If this is not the case, price volatility may decrease, reducing the potential for arbitrage and, consequently, energy cost savings. Therefore, the *lower bound* of the energy cost savings potential is zero. Research has also shown that large numbers of price-responsive loads could destabilize the system [11], [12]

The following section describes and compares the three models and two optimization/control frameworks considered in this work. Section III presents simulation results and Section IV summarizes our conclusions.

II. METHODS

We describe three TCL aggregation models and two optimization/control frameworks used to explore the energy arbitrage problem. Table I summarizes the models that we will introduce in this section. For each framework, we list which models were used (1) as the plant (i.e. the “real system”), (2) within the optimization algorithm, and (3) within the control algorithm.

A. Model 1: Aggregation of Individual TCL Models

Model 1 is a high fidelity model used as the plant within each framework. A direct way to model an aggregation of heterogenous TCLs is to simulate thousands of individual TCLs using the first-order model developed in [13], [14], [15]. In this model, each TCL’s temperature state evolution is described with a stochastic hybrid discrete time difference equation:

$$\theta_{k+1}^i = a^i \theta_k^i + (1 - a^i)(\theta_{a,k}^i - q_k^i \theta_g^i) + \epsilon_k^i, \quad (1)$$

where θ_k^i is the internal temperature of TCL i at time step k , θ_a is the ambient temperature, and ϵ is a noise process. The dimensionless TCL parameter a^i is defined as $e^{-h/(C^i R^i)}$, where C^i is a TCL’s thermal capacitance, R^i is its thermal resistance, and h is the model time step. θ_g^i is the temperature gain when a TCL is on and is equal to $R^i P_{\text{trans}}^i$, where P_{trans}^i is a TCL’s energy transfer rate, which according to our conventions is positive for cooling TCLs and negative for heating TCLs. P^i is defined as the power consumed by TCL i when it is on, and is equal to $|P_{\text{trans}}^i|/\text{COP}^i$, where COP^i is its coefficient of performance. The local control variable q^i is a dimensionless discrete variable equal to 1 when the TCL is on and 0 when the TCL is off. For cooling TCLs, it evolves as follows:

$$q_{k+1}^i = \begin{cases} 0, & \theta_{k+1}^i < \theta_{\text{set}}^i - \delta^i/2 \\ 1, & \theta_{k+1}^i > \theta_{\text{set}}^i + \delta^i/2 \\ q_k^i, & \text{otherwise} \end{cases} \quad (2)$$

where θ_{set}^i is the temperature set point and δ^i is the dead-band width. For heating TCLs, the position of the 0 and 1 are switched.

We assume that a centralized direct load controller can switch loads on or off while the loads are within their temperature dead-band; however, it can not change a TCL’s temperature directly or affect its temperature set point. Additionally, we assume TCLs become uncontrollable if they are outside of the dead-band. These assumptions ensure that the control is non-disruptive, i.e., TCLs stay within their existing dead-bands.

TCLs with compressors, such as air conditioners and refrigerators, should not be cycled on/off too quickly or else the compressor may fail. While this constraint is not explicitly included in the individual TCL model, the external controller can be designed to minimize the chance of compressor short-cycling, for example, by preferentially switching TCLs that are about to switch and/or not allowing TCLs in certain states to switch.

For arbitrage, we aim to minimize energy costs over a time horizon. We could develop an optimal controller based on Model 1 that would allow us to control each TCL individually; however, this would require significant local computational capabilities or knowledge of individual TCL parameters by the central controller. This motivates the development of alternative models and control/optimization frameworks, discussed in the next subsections.

B. Model 2: Extended State Bin Transition Model

Since it would be computationally intractable to use Model 1 for optimal control, we instead consider a simplified aggregate system model, the state bin transition model [16], [17], [18], which is similar to models developed in [19], [20], [21], [22]. The benefit of this model is that it is linear and therefore lends itself to easy application of control and optimization techniques. Moreover, it is good at short timescale (e.g., seconds) prediction [18]. Here, we investigate its potential for longer timescale prediction and optimization. However, to apply it to this problem, we extended it in two important ways, described below.

In the state bin transition model, all TCLs within a heterogenous TCL population divide their dead-band into m equal-sized temperature intervals (thus, the interval length may be different for each TCL). We then assign two state bins to each temperature interval, one to the on state and one to the off state. The state vector x contains the fraction of TCLs in each state bin. Our first extension to the model is to include two extra bins to keep track of TCLs outside the dead-band, similar to in [23]. We referred to these extra bins as “outside bins,” and with these bins $x \in \mathbb{R}^n$ where $n = 2m + 2$. A TCL is only switched after it has left its dead-band and so at any instant in time some TCLs will be outside of their dead-bands and these TCLs are uncontrollable. Moreover, some TCLs may be outside of their dead-bands because of the ambient temperature. Including the outside bins allows us to keep track of the

TABLE I
THREE TCL AGGREGATION MODELS

	Model 1	Model 2	Model 3
System type	hybrid	linear	linear
Order	N_p , the number of TCLs	10-100	1
System knowledge/identification requirements	individual TCL parameters	aggregate system parameters	energy/power capacity limits
Framework 1 models	plant	optimization/control	-
Framework 2 models	plant	control	optimization

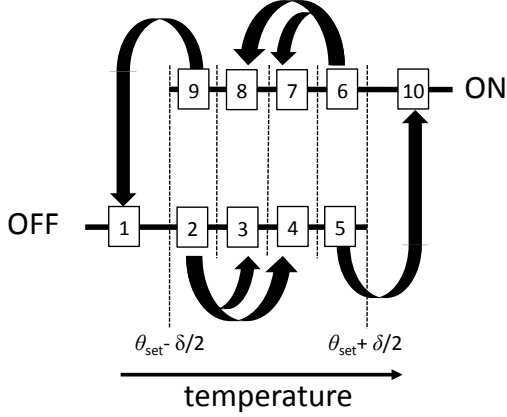


Fig. 1. Discretized dead-band used in the extended state bin transition model ($n = 10$) for cooling TCLs. Not all possible transitions are shown.

TCLs that are uncontrollable. Figure 1 shows the discretized dead-band including the outside bins.

The discrete time motion of TCLs around the discretized state space can be described by a Markov transition matrix, the transpose of which is the A -matrix commonly used in control applications. In previous work, the A -matrix was derived/identified given a fixed ambient temperature; however, for energy arbitrage with air conditioners and space heaters it is important to model the system over time periods of hours in which the ambient temperature changes. Therefore, our second extension is to transform the linear time-invariant model into a linear time-varying model:

$$x_{k+1} = A_k x_k + B u_k \quad (3)$$

$$y_k = C_k x_k, \quad (4)$$

where $A_k = A(\theta_{a,k}) \in \mathbb{R}^{n \times n}$.

We assume that we can control TCLs within the dead-band by turning them on or off. Thus, we define an input $u \in \mathbb{R}^m$. The absolute value of each entry of u is the fraction of the total TCLs in the system to be turned on/off from a temperature interval. Negative values of u turn TCLs off, while positive values turn TCLs on. Corresponding to the bin numbering in Figure 1, $B \in \mathbb{R}^{n \times m}$ is as follows:

$$B = \begin{bmatrix} 0_{1 \times m} \\ -I_{m \times m} \\ J_{m \times m} \\ 0_{1 \times m} \end{bmatrix},$$

where J is an anti-diagonal matrix with ones on the anti-diagonal. The choice of B ensures that we do not control

TCLs in the outside bins, and that TCLs that switch from an on bin end up in the corresponding off bin and vice versa.

The output measurement, y , is simply the aggregate power consumption of the TCL population, which is computed by defining $C \in \mathbb{R}^n$ as follows:

$$C_k = N_p \bar{P}_{ON,k} [\mathbf{0}_{1 \times (m+1)} \quad \mathbf{1}_{1 \times (m+1)}],$$

where N_p is the number of TCLs in the aggregation and \bar{P}_{ON} is the mean power consumption of TCLs in the on state. We allow \bar{P}_{ON} to vary as a function of θ_a , but assume that for a given θ_a it is constant, and we compute it through system identification. In general, $\bar{P}_{ON,k} \approx \bar{P}$.

To minimize communication from the central controller to the TCLs, we divide the entries of u by the relevant entries of x to create a control vector of “switch probabilities” u_{rel} , which we broadcast to all TCLs. TCLs decide whether or not to switch probabilistically, by comparing a random number drawn from a uniform distribution between 0 and 1 to the entry of u_{rel} corresponding to their current state. Note that if we have a poor estimate of x our control may be poor [18]; however, here we assume we know x .

For system identification purposes, we assume A_k belongs to a finite number of matrices A_1, A_2, \dots, A_{N_a} , each associated with a specific θ_a . To identify $A(\theta_a)$, we run Model 1 in steady state at θ_a and count the number of transitions from bin-to-bin over time. Empirically, we find that the A -matrices are related to each other; plotting specific entries of A as a function of θ_a we find near linear relationships. This observation may be useful for identifying a real system. Specifically, we could identify A -matrices for only a small set of θ_a and then additional A -matrices could be interpolated/extrapolated. This idea will be explored in the future.

C. Framework 1: Optimal Control with Model 2

In Framework 1, we use Model 2 to formulate a receding horizon linear program (LP). Though Model 2 is used to formulate the optimal controller, the control inputs are applied to the plant (Model 1).

Let L_j denote the energy price during price interval j : $[t, t + \Delta T]$, for example, $\Delta T = 5$ minutes as in the California Independent System Operator (CAISO) real-time market considered in Section III. In general, $\Delta T \neq h$. The price paid for energy consumed in interval j is $L_j \bar{P}_{agg,j} \Delta T$ where $\bar{P}_{agg,j}$ is the mean power consumed by the TCLs in the interval. We create a higher resolution price signal, l ; specifically, $l_k = L_j$ for $k = t, t + h, \dots, t + \Delta T - h$. Denote $N_t = \frac{\Delta T}{h}$. Then, the price paid during the interval is $h \sum_{k=t}^{t+N_t} l_k y_k$. Let $[t, t + N]$ denote the optimization

planning horizon, over which we have forecasts of L_j and θ_a . To minimize energy costs, we formulate the following optimization problem:

$$\begin{aligned} \min_{u \in U} h \sum_{k=t}^{t+N} l_k y_k \quad (5) \\ \text{s.t. } H_l x_k \leq u_k \leq H_u x_k, (3), \text{ and } (4), \end{aligned}$$

where we assume x_k is known, $U = [-1, 1]^{N \times m}$, and $H_l, H_u \in \mathbb{R}^{m \times n}$ are defined such that each element of u is constrained: $-x_{n-s} \leq u_s \leq x_{s+1}$, meaning that in each temperature interval we can switch *off* a fraction of TCLs equal to or less than the total fraction of TCLs in the *on* bin associated with that temperature interval and vice versa. The optimization problem is an LP, and can be solved as a receding-horizon control problem.

We implemented the optimal controller and found that Model 2 predicts unrealistic energy savings. When price volatility is low, the optimization tends to push TCLs towards the “low-energy” edge of the dead-band ($\theta \sim \theta_{\text{set}} + \delta/2$ for cooling TCLs and $\theta \sim \theta_{\text{set}} - \delta/2$ for heating TCLs) to minimize energy consumption and therefore energy costs. Unfortunately, since Model 2 is identified when the system is operating in steady state, model performance when the system is pushed to its limits is poor. Specifically, transition probabilities into and out of the outside bins change when all TCLs operate at the dead-band edge because TCLs are not distributed uniformly in the bins.

A consequence of this issue is that Model 2 underestimates the amount of energy consumed by the system when all TCLs operate at the low-energy edge of the dead-band. In Fig. 1, consider a population of air conditioners forced to operate near $\theta_{\text{set}} + \delta/2$. Consider a TCL in bin 10; as soon it switches into bin 6, the controller turns it off and it goes to bin 5. In this scenario, it is more likely for TCLs in bin 6 to be closer to the dead-band edge than the boundary between bins 5 and 6. However, when we switch TCLs into bin 5, Model 2 “loses” their positions within the bin and instead assumes they are distributed as in steady state. This increase in thermal energy obviously does not exist in a real system (or in Model 1). To mitigate this issue, we could increase the number of bins; however, the receding-horizon LP soon becomes non-computable in real time.

Over short prediction horizons (e.g., 15 minutes), energy savings opportunities often outweigh price arbitrage opportunities, and so TCLs spend much of their time operating near the edge of the dead-band, which would not be possible in a real system because of compressor short-cycling. This also results in model mismatch, incorrect control inputs that can cause the system to be pushed in the wrong direction, and a lack of energy cost savings. Increasing the prediction horizon mitigates this issue; however, again, the receding-horizon LP soon becomes intractable. This finding motivated our development of Model 3 and Framework 2.

D. Model 3: Time-varying Thermal Battery Model

Model 3 is used to compute near-optimal control trajectories. The model’s simplicity makes optimization computa-

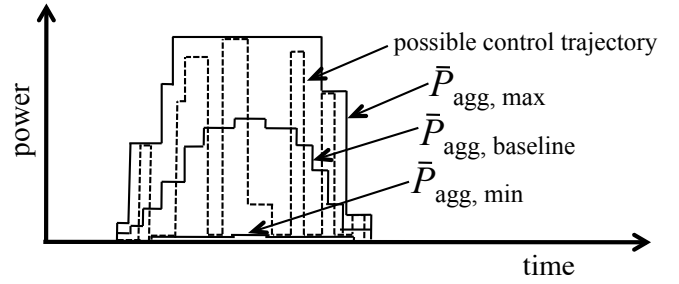


Fig. 2. A TCL population’s baseline and power constraints. The TCL population also has energy constraints, not shown.

tionally tractable in real time but the model is not useful for control algorithm development because it does not take into account the detailed system dynamics. Instead it keeps track of a TCL population’s energy state, S_j , as a function of its mean aggregate power usage, \bar{P}_{agg} , in each price interval, j , of width ΔT . An energy state is similar to a battery’s state of charge; it describes how full an energy storage unit is. Without external control, a TCL population’s time-varying power trajectory is referred to as its “baseline.” Figure 2 shows a TCL population’s mean aggregate power baseline, $\bar{P}_{\text{agg, baseline}}$, over a day. A TCL population increases its energy state when $\bar{P}_{\text{agg},j} > \bar{P}_{\text{agg, baseline},j}$, and decreases it when $\bar{P}_{\text{agg},j} < \bar{P}_{\text{agg, baseline},j}$:

$$S_{j+1} = S_j + (\bar{P}_{\text{agg},j} - \bar{P}_{\text{agg, baseline},j})\Delta T. \quad (6)$$

As shown in Fig. 2, the choice of $\bar{P}_{\text{agg},j}$ is constrained:

$$\bar{P}_{\text{agg, min},j} \leq \bar{P}_{\text{agg},j} \leq \bar{P}_{\text{agg, max},j}. \quad (7)$$

S is also constrained:

$$0 \leq S_j \leq S_{\text{max},j}. \quad (8)$$

These bounds define the *power and energy capacities* of a TCL population. They are time varying quantities because they are a function of the number of TCLs that are “available” for control. A TCL is available if it is operating within its dead-band. When $\bar{P}_{\text{agg}} = \bar{P}_{\text{agg, min}}$, all available TCLs are off, while when $\bar{P}_{\text{agg}} = \bar{P}_{\text{agg, max}}$, all available TCLs are on. When $S = 0$ the thermal battery is depleted meaning all available TCLs operate at one edge of the dead-band (e.g., for cooling TCLs all operate near $\theta_{\text{set}} + \delta/2$). When $S = S_{\text{max}}$, the thermal battery is full meaning all available TCLs operate at the other edge of the dead-band.

Here, we assume cooling TCLs are available when $\theta_a > \theta_{\text{set}}^i + \delta^i/2$ and $\theta_a - R^i P_{\text{trans}}^i < \theta_{\text{set}}^i - \delta^i/2$. The first inequality requires that the ambient temperature be greater than the upper edge of the dead-band. The second requires that the TCL is able to cool the space to within the dead-band. In a real system, thermal inertia and internal gains lead to differences between internal and ambient temperatures and so TCLs may not be available when we expect them to be. Moreover, control actions affect TCL availability. This results in model mismatch.

To use Model 3, we need to derive or identify $\bar{P}_{\text{agg, baseline}}$, $\bar{P}_{\text{agg, min}}$, $\bar{P}_{\text{agg, max}}$, and S_{max} . These parameters are a function

of ambient temperature dynamics, but for simplicity we assume that each is simply a function of the current ambient temperature, θ_a . Additionally, we assume that each belongs to a finite set of values and develop a look-up table that specifies an estimate of each value as a function of θ_a .

If we know all TCL parameters, we can estimate $\bar{P}_{\text{agg, baseline}}$ and S_{max} directly. We first define a TCL's duty cycle for fixed θ_a :

$$\Delta^i = \frac{h_{\text{ON}}^i}{h_{\text{ON}}^i + h_{\text{OFF}}^i} \quad (9)$$

where h_{ON} and h_{OFF} represent the time it takes for a TCL to travel from one end of the dead-band to the other in the on state and the off state, respectively. They are defined as:

$$h_{\text{ON}}^i = -R^i C^i \ln \frac{\theta_{\text{set}}^i - \delta^i/2 - \theta_a^i + \theta_g^i}{\theta_{\text{set}}^i + \delta^i/2 - \theta_a^i + \theta_g^i} \quad (10)$$

$$h_{\text{OFF}}^i = -R^i C^i \ln \frac{\theta_{\text{set}}^i + \delta^i/2 - \theta_a^i}{\theta_{\text{set}}^i - \delta^i/2 - \theta_a^i} \quad (11)$$

Only positive values of h_{ON}^i and h_{OFF}^i are used to compute Δ^i . When h_{ON}^i is negative, the TCL is unavailable and $\Delta^i = 1$, and when h_{OFF}^i is negative, the TCL is also unavailable but $\Delta^i = 0$.

$\bar{P}_{\text{agg, baseline}}$ is estimated as follows:

$$\bar{P}_{\text{agg, baseline}} = \sum_{i=1}^{N_p} \bar{P}_{\text{baseline}}^i \quad (12)$$

where, for cooling TCLs,

$$\bar{P}_{\text{baseline}}^i = \begin{cases} P^i \Delta^i, & \text{if available} \\ 0, & \text{otherwise} \end{cases} \quad (13)$$

S_{max} is estimated as follows:

$$S_{\text{max}} = \sum_{i=1}^{N_p} S_{\text{max}}^i \quad (14)$$

where, for cooling TCLs,

$$S_{\text{max}}^i = \begin{cases} P^i h_{\text{ON}}^i (1 - \Delta^i), & \text{if available} \\ 0, & \text{otherwise} \end{cases} \quad (15)$$

If we do not know the individual TCL parameters, we can not estimate $\bar{P}_{\text{agg, baseline}}$ and S_{max} with (12)-(15), but we can estimate them through system identification. Additionally, we must identify $\bar{P}_{\text{agg, min}}$ and $\bar{P}_{\text{agg, max}}$ because there is no straightforward way to compute these quantities. Here, we identify these parameters using the simulated output of Model 1 though, in principle, this could be done with a real population of TCLs.

We identify each parameter for each θ_a by starting Model 1 in steady state at θ_a . $\bar{P}_{\text{agg, baseline}}$ is simply the aggregate power consumed by the TCLs. To compute $\bar{P}_{\text{agg, max}}$, we force each available TCL to be on at each model time step k over an interval of length ΔT , and then compute the average power over the interval. Because this forcing will cause increasingly more TCLs to be outside of the dead-band (and

therefore uncontrollable), the aggregate power consumption will decrease over time. We compute $\bar{P}_{\text{agg, min}}$ similarly by turning TCLs off at each model time step and then computing the average power over the interval.

Identifying S_{max} requires determining the amount of energy associated with all TCLs moving from one side of the dead-band to the other. Starting with the system in steady state, we can force each TCL in the dead-band to be on until all TCLs are at one edge of the dead-band and we loose control of the the TCL population in that direction. S_{up} is the integral of the power consumed by the system referenced to $\bar{P}_{\text{agg, baseline}}$, from the onset of forcing until we loose control. S_{down} is determined similarly by forcing the TCLs off until all are at the other edge of the dead-band and we loose control. S_{max} is $S_{\text{up}} + S_{\text{down}}$.

E. Framework 2: Decoupled Optimization and Control

In Framework 2, we use Model 3 for optimization and Model 2 for control. While Model 2 is unsuitable for optimal control, as described above, it performs well for tracking control [18]. This decoupled approach can be thought of as similar to approaches commonly used in aviation path planning [24].

We aim to determine the optimal mean aggregate power consumption in each interval, \bar{P}_{agg}^* , and so we solve:

$$\begin{aligned} \min \Delta T \sum_{j=t}^{t+N} L_j \bar{P}_{\text{agg},j} \\ \text{s.t. (6), (7), and (8),} \end{aligned} \quad (16)$$

which can be solved as a receding-horizon LP. We then transform \bar{P}_{agg}^* into a control trajectory p_{agg}^* with the correct time step; specifically, $p_{\text{agg},k}^* = \bar{P}_{\text{agg},j}^*$ for $k = t, t+h, \dots, t+\Delta T - h$.

Model 2 is used to track p_{agg}^* with the predictive proportional controller (PPC) proposed in [18]. Our goal is to calculate u_{goal} , the total fraction of TCLs to switch on or off in the next time step. First, we compute:

$$u'_{\text{goal},k} = \frac{p_{\text{agg},k+1}^* - y_{k+1}}{N_p \bar{P}_{\text{ON},k}}, \quad (17)$$

where y_{k+1} is computed with (3) and (4). Then, $u_{\text{goal},k}$ is calculated by putting $u'_{\text{goal},k}$ through a saturation filter with minimum equal to the fraction of TCLs on, $-\sum_{s=m+2}^n x_{s,k}$, and maximum equal to the fraction of TCLs off, $\sum_{s=1}^{m+1} x_{s,k}$. The saturation filter introduces error in the control but ensures that we do not attempt to switch more TCLs than are available to switch. u_{goal} can be distributed to the bins in different ways, for example, equally or by preferentially switching TCLs that are about to switch. Here we do the latter, for example, in the 10 bin system in Fig. 1, if the controller needed to switch TCLs on, it would switch TCLs in bin 5 preferentially over TCLs in bin 4, and so on. This helps minimize the chance of compressor short-cycling; however, when the system attempts to minimize energy consumption this could still occur. To solve this problem, we could constrain the bins to which we apply

TABLE II
AIR CONDITIONER PARAMETERS*

θ_{set}	temperature setpoint	18–27°C
δ	temperature dead-band width	0.25–1°C
R	thermal resistance	1.5–2.5°C/kW
C	thermal capacitance	1.5–2.5 kWh/°C
P_{trans}	energy transfer rate	10–18 kW
COP	coefficient of performance	2.5
ϵ	model noise	$\mathcal{N}(0, 5 \times 10^{-4})$
h	model time step	10 s

*verified against real data from California, USA in [4]

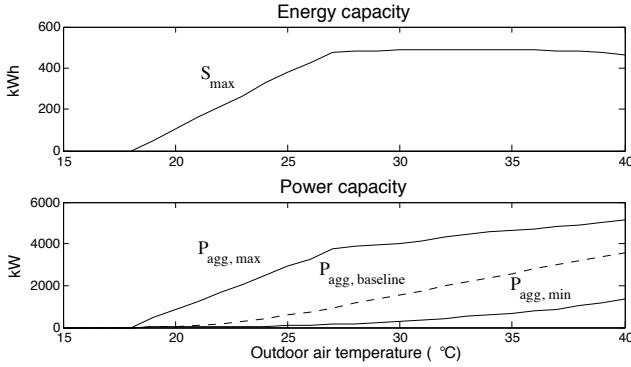


Fig. 3. Energy and power capacity of a population of air conditioners as a function of outdoor air temperature.

control, for example, never applying control to bins 2 or 6; however, this would decrease S_{max} . Another solution could be to design a more advanced controller that could determine the optimal distribution of control to the bins based on costs and constraints, as in [16].

III. RESULTS

We implemented Framework 2 in simulation and solved the deterministic problem to determine the upper bound of the energy cost savings potential. In this section, we describe the simulation setup, results for the deterministic problem, and some insights into the stochastic problem.

A. Simulation Set-up

For all simulations, we used $N_p = 1,000$ central air conditioners parameterized with the values in Table II. Specifically, we randomly drew parameters from uncorrelated uniform distributions between the minimum and maximum values shown. Using the system identification methodology described in Section II-D, we determined the TCL population’s energy and power capacity as a function of the current outdoor air temperature, as shown in Fig. 3.

We use $n = 42$ bins in Model 2. For the deterministic problem, we perform one optimization each day, i.e. $N = 24$ hours, and assume perfect price and temperature forecasts. We used one full year (2010) of data from Merced, California, USA: 5-minute energy market prices (interval locational marginal prices) from CAISO node MERCED.1_N001 [25] and outdoor air temperature data from NOAA weather station Merced 23 WSW [26]; statistics are shown in Table III. We linearly interpolated the temperature data for use in Model 1;

TABLE III
5-MINUTE ENERGY PRICE AND OUTDOOR AIR TEMPERATURE
STATISTICS (MERCED, CALIFORNIA, USA 2010)

	mean	median	min	max	std
price (\$/MWh)	39.15	33.88	-240.81	793.13	61.07
temperature (°C)	15.0	13.1	-4.6	39.6	8.3

however, we identified $\bar{P}_{\text{agg, baseline}}$, $\bar{P}_{\text{agg, min}}$, $\bar{P}_{\text{agg, max}}$, S_{max} , A , and \bar{P}_{ON} only for integer values of temperature and, at each time step, used the parameter values associated with the closest integer temperature. In principle, we could also interpolate these values.

To ensure that energy cost savings are primarily due to arbitrage as opposed to energy savings resulting from the controller forcing TCLs to operate at the edge of the dead-band, we simulated a system constrained to operate at the edge of the dead-band with $\delta = 0$ and found that it consumes 4.9% less energy and saves 5.4% in energy costs over the course of the year as compared to the system operating normally. These values are useful for comparison to those in the next section; in reality one would not be able to operate the system in this way because of compressor short-cycling.

B. Results for the Deterministic Problem

The results of the optimization problem predict that a population of air conditioners in Merced could save, at most, 17% in wholesale energy cost through arbitrage in CAISO’s 5-minute energy market. When we control the population to track the optimal trajectory, we find maximum savings are closer to 14%, specifically the uncontrolled population would have spent about \$91,500 for energy during the year while the same population doing energy arbitrage would have spent \$78,400. This translates to about \$13 in wholesale energy cost savings per TCL per year. Since this analysis assumes perfect price and weather forecasts and exogenous electricity prices, this is an upper bound on the potential energy costs savings in Merced, assuming future prices and price volatility are similar to those in the past. Ultimately, an aggregator would need to decide if arbitrage revenues could be sufficient to cover upfront costs including hardware, software, and installation; reoccurring costs including operations, maintenance, and incentive payments to customers; and its desired profit margin.

In Fig. 4, we break down the results and show histograms containing the population’s daily energy cost savings (for days with savings over \$10) over the course of the year, both as predicted by the optimization and after tracking control. More than 200 days per year have little-to-no potential for energy cost savings, in most cases because outdoor air temperatures are low and so the air conditioners are not used much or at all. The optimization is always optimistic in its prediction of energy cost savings; in reality the TCL population is not able to closely follow the optimal trajectory because of mismatch between Model 1 and Models 2 and 3, shown in Fig. 5. Despite the issues associated with using Model 2 for optimization, we have found that using it for

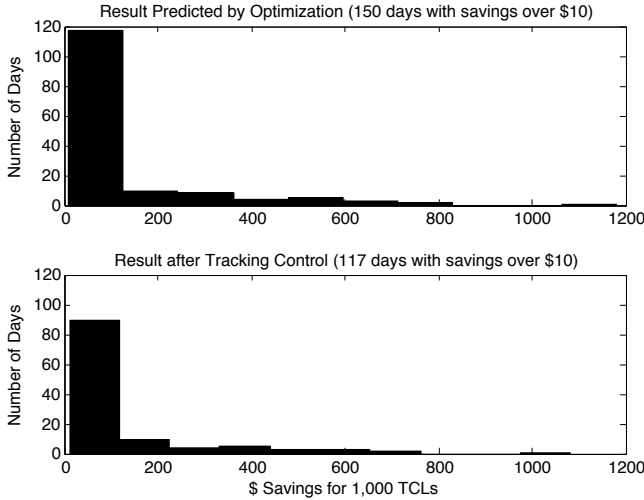


Fig. 4. Histograms showing daily energy cost savings for a population of 1,000 air conditioners, given outdoor air temperatures and 5-minute energy market prices in Merced, California, USA in 2010. The mean daily energy cost for the uncontrolled population considering only days with over \$10 in possible energy cost savings is \approx \$710.

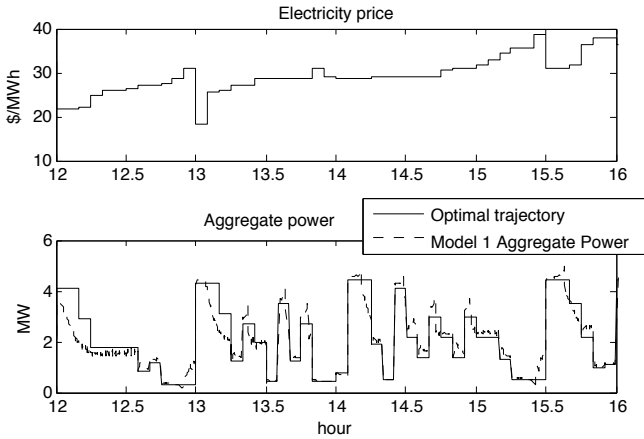


Fig. 5. Model 1 tracking the desired trajectory.

TCL population control results in higher energy cost savings than using a model-free proportional controller.

C. Results for the Stochastic Problem

To explore stochastic problems, we analyze just one day (Sept. 3) with a mean outdoor air temperature of 24.1°C , optimization-predicted energy cost savings of 28.4%, and energy cost savings after tracking control of 27.2%. We first examine the effect of stochasticity in price forecasts. We model the price forecast, L_f , as follows:

$$L_{f,j} = L_j + w_j, \quad (18)$$

where L are the real price data and w is the price forecast error modeled as an autoregressive process, $w_{j+1} = \gamma w_j + \alpha \epsilon_j$, where ϵ is Gaussian white noise with standard deviation 1, and $w_1 = 0$, since we always know the current price. We solve the deterministic LP using noisy price forecasts and

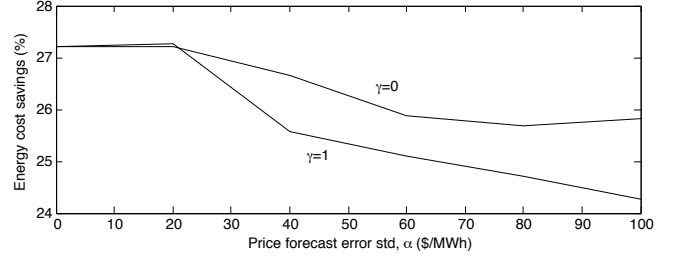


Fig. 6. Energy cost savings as a function of price forecast error standard deviation, for $\gamma = 0, 1$. Other possible γ -trajectories are between those shown.

$N = 1$ hour. We repeat the optimization every 5 minutes, keeping only the first value of \bar{P}_{agg}^* each time. The controller attempts to follow the trajectory and then we compute energy cost savings with the real price data.

We ran 10 Monte Carlo simulations for various α and γ and show the energy cost savings (after tracking control) in Fig. 6. We use very large values of α because of the large range of prices on that day, $\$-37.44$ to $\$767.78$ per MWh, with mean price $\$47.47$ per MWh. For this day, small amounts of uncertainty do not affect the results very much, but as α and γ increase further, the savings decrease.

We also briefly explored the effect of ambient temperature forecast uncertainty, which causes model mismatch. Over horizons of less than a few hours, we can forecast ambient temperatures fairly well and so we assumed modest levels of uncertainty. We found that while temperature forecast uncertainty can decrease energy cost savings, the effect is small compared to that of price forecast uncertainty.

Lastly, we explored the effect of mismatch in the way that the control is modeled and implemented. In a real system, it would be desirable to design the control so that switching actions are never sent to TCLs that have just switched, which ensures that the compressors do not short-cycle. However, this constraint is not explicitly included in Model 3, resulting in more mismatch between Models 3 and 1. We investigated this scenario by never allowing switching from bins 2 – 11 and 22 – 31, and found that energy cost savings decreased from 27.2% to 21.1%. It is possible that improving Model 3 to reflect this constraint could improve the energy cost savings.

IV. CONCLUDING REMARKS

In this paper, we explored the potential for TCL aggregations to arbitrage intra-hour electricity market prices via non-disruptive direct load control. We presented three TCL aggregation models and two optimization/control frameworks for the energy arbitrage problem. Our investigation provides insight into the applicability of each model. Due to modeling and computational issues associated with the first framework, we developed the second framework in which we decoupled the optimization and control problems and used different models to solve each. Specifically, we developed a time-varying thermal battery model and used it to compute the

optimal trajectory and we extended the state bin transition model and used it to develop the control algorithm.

We find that a population of air conditioners participating in energy arbitrage in CAISO's 5-minute energy market in Merced could save, at most, 14% of wholesale energy costs, which translates to about \$13 per TCL per year. In locations where air conditioners are more heavily used and/or intra-day electricity market prices are more volatile (e.g., future electricity markets with more intermittent renewable resources), the potential savings would be higher. Ultimately though, the ability of a load aggregator to profit from arbitrage is a function of its ability to forecast prices and temperatures and the effect of its actions on the market prices. As we have shown, stochasticity reduces energy cost savings potentials, making realistic energy cost savings seem rather modest. A load aggregator would need to determine if expected revenues would provide sufficient profit after covering the costs associated with TCL control, e.g., hardware, software, operations & maintenance, and compensation to the TCL owners.

Future work could consider other opportunities for TCL participation in energy markets, e.g., ancillary service market participation may be more lucrative [4]. Future work could also consider more realistic models [27] and the design of a receding horizon controller that takes into account stochasticity. Additionally, it could consider the effects of user behavior on energy cost savings and ways to explicitly account for the effect of real-world constraints, such as compressor lock-out (which helps TCLs avoid short-cycling), on TCL population's energy/power capacities.

V. ACKNOWLEDGMENT

The authors would like to thank Mark Dyson, Josh Taylor, and Wei Zhang for helpful discussions.

REFERENCES

- [1] D. Callaway and I. Hiskens, "Achieving controllability of electric loads," *Proceedings of the IEEE*, vol. 99, no. 1, pp. 184–199, 2011.
- [2] H. Wellinghoff, D. Morenoff, J. Pederson, and M. Tighe, "Creating regulatory structures for robust demand response participation in organized wholesale electric markets," in *Proceedings of ACEEE Summer Study on Energy Efficiency in Buildings*, Pacific Grove, CA, 2008.
- [3] J. Taneja, D. Culler, and P. Dutta, "Towards cooperative grids: sensor/actuator networks for renewables integration," in *Proceedings of IEEE SmartGridComm*, Gaithersburg, MD, 2010.
- [4] J. Mathieu, M. Dyson, and D. Callaway, "Using residential electric loads for fast demand response: The potential resource and revenues, the costs, and policy recommendations," in *Proceedings of the ACEEE Summer Study on Buildings*, Pacific Grove, CA, Aug. 2012.
- [5] S. Vosen and J. Keller, "Hybrid energy storage systems for stand-alone electric energy stems: optimization of system performance and cost through control strategies," *International Journal of Hydrogen Energy*, no. 24, pp. 1139–1156, 1999.
- [6] R. Walawalkar, J. Apt, and R. Mancini, "Economics of electric energy storage for energy arbitrage and regulation in new york," *Energy Policy*, no. 35, pp. 2558–2568, 2007.
- [7] P. Denholm and R. Sioshansi, "The value of compressed air energy storage with win in transmission constrained electric power systems," *Energy Policy*, no. 37, pp. 3149–3158, 2009.
- [8] R. Sioshansi, P. Denholm, T. Jenkin, and J. Weiss, "Estimating the value of electricity storage in PJM: Arbitrage and some welfare effects," *Energy Economics*, no. 31, pp. 269–277, 2009.
- [9] V. Marano, G. Rizzo, and F. Tiano, "Application of dynamic programming to the optimal management of a hybrid power plant with wind turbines, photovoltaic panels and compressed air energy storage," *Applied Energy (in press)*, 2012.
- [10] J. Taylor, D. Callaway, and K. Poolla, "Competitive energy storage in the presence of renewables," *IEEE Transactions on Power Systems (in review)*, 2012.
- [11] M. Roozbehani, M. Dahleh, and S. Mitter, "Volatility of power grids under real-time pricing," *IEEE Transactions on Power Systems (in press)*, 2012.
- [12] M. Negrete-Pincetic and S. Meyn, "Intelligence by design for the entropic grid," in *Proceedings of IEEE PES General Meeting*, Detroit, MI, 2011.
- [13] S. Ihara and F. Schweppe, "Physically based modeling of cold load pickup," *IEEE Transactions on Power Apparatus and Systems*, vol. PAS-100, no. 9, pp. 4142–4150, 1981.
- [14] R. Mortensen and K. Haggerty, "Dynamics of heating and cooling loads: models, simulation, and actual utility data," *IEEE Transactions on Power Systems*, vol. 5, no. 1, pp. 243–249, 1990.
- [15] C. Uçak and Çağlar, "The effect of load parameter dispersion and direct load control actions on aggregated load," in *Proceedings of POWERCON '98*, vol. 1, 1998, pp. 280–284.
- [16] S. Koch, J. Mathieu, and D. Callaway, "Modeling and control of aggregated heterogeneous thermostatically controlled loads for ancillary services," in *Proceedings of the Power Systems Computation Conference*, Stockholm, Sweden, Aug. 2011.
- [17] J. Mathieu and D. Callaway, "State estimation and control of heterogeneous thermostatically controlled loads for load following," in *Proceedings of the Hawaii International Conference on Systems Science*, Wailea, HI, Jan. 2012, pp. 2002–2011.
- [18] J. Mathieu, S. Koch, and D. Callaway, "State estimation and control of electric loads to manage real-time energy imbalance," *IEEE Transactions on Power Systems*, 2012.
- [19] N. Lu, D. Chassin, and S. Widergren, "Modeling uncertainties in aggregated thermostatically controlled loads using a state queueing model," *IEEE Transactions on Power Systems*, vol. 20, no. 2, pp. 725–733, 2005.
- [20] N. Lu and D. Chassin, "A state queueing model of thermostatically controlled appliances," *IEEE Transactions on Power Systems*, vol. 19, no. 3, pp. 1666–1673, 2004.
- [21] S. Bashash and H. Fathy, "Modeling and control insights into demand-side energy management through setpoint control of thermostatic loads," in *American Control Conference*, 2011, pp. 4546–4553.
- [22] S. Kundu, N. Sinityn, S. Backhaus, , and I. Hiskens, "Modeling and control of thermostatically controlled loads," in *Proceedings of 17th Power Systems Computation Conference*, Stockholm, Sweden, Aug 2011.
- [23] K. Kalsi, M. Elizondo, J. Fuller, S. Lu, and D. Chassin, "Development and validation of aggregated models for thermostatic controlled loads with demand response," in *Proceedings of Hawaii International Conference on Systems Science*, Wailea, HI, 2012.
- [24] M. Kamgarpour, V. Dadok, and C. Tomlin, "Trajectory generation for aircraft subject to dynamic weather uncertainty," in *IEEE Conference on Decision and Control*, Atlanta, GA, 2010.
- [25] CAISO, "Open access same-time information system site," California Independent System Operator, 2012. [Online]. Available: <http://oasis.caiso.com>
- [26] NOAA, "National climatic data center: US climate reference network data set: Merced 23 WSW," National Oceanic and Atmospheric Administration, 2010. [Online]. Available: http://www1.ncdc.noaa.gov/pub/data/uscrn/products/hourly02/2010/CRNH0202-2010-CA_Merced_23_WSW.txt
- [27] W. Zhang, K. Kalsi, J. Fuller, M. Elizondo, and D. Chassin, "Aggregate model for heterogeneous thermostatically controlled loads with demand response," in *Proceedings of IEEE PES General Meeting*, San Diego, CA, 2012.